ACS OMEGA

http://pubs.acs.org/journal/acsodf

Article

# Novel Method for the Production of Titanium Foams to Reduce Stress Shielding in Implants

Khurram Yaqoob,* Izza Amjad, Muhammad Awais Munir Awan, Usman Liaqat, Muhammad Zahoor, and Muhammad Kashif

Cite This: *ACS Omega* 2023, 8, 1876−1884

Read Online

ACCESS | Metrics & More | Article Recommendations

**ABSTRACT:** Titanium foams have potential applications in orthopedic and dental implants because of their low elastic modulus and good bone in-growth properties. In the present study, a novel method for the preparation of three-dimensional interconnected microporous titanium foams has been developed. This method is based on the insertion of a filler metal into the titanium metal by arc melting, followed by its removal by an electrochemical dealloying process for the development of foams. Complete removal of the filler metal by the electrochemical dealloying process was confirmed by an X-ray diffractometry (XRD) analysis, whereas scanning electron microscopy (SEM) analysis of the developed foams showed the development of interconnected porosity. Ti foams with different levels of porosities were successfully developed by varying the amount of the filler metal. Mechanical and thermal characterizations of the developed foams were carried out using compression testing and laser flash apparatus, respectively. The yield strength and elastic modulus of the developed foams were found to decrease by increasing the volume fraction of pores. The elastic modulus of the developed titanium foams (15.5−36 GPa) was found to be closer to that of human bones, whereas their yield strength (147−170 MPa) remained higher than that of human bones. It is therefore believed that the developed Ti foams can help in reducing the problem of stress shielding observed in orthopedic implants. The thermal diffusivity of the developed foams (4.3−0.69 $mm^2/s$) was found to be very close to that of human dentine.

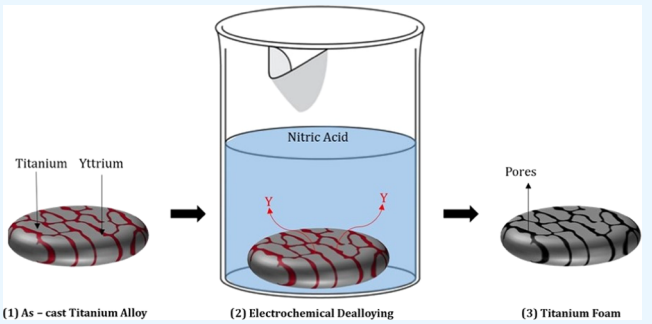


## INTRODUCTION

An ideal implant material must possess the optimum combination of biological, mechanical, and thermal properties.[1] Biocompatibility is required to achieve an ideal interaction between the body and the implant.[2] The optimum combination of mechanical properties is required for the shaping of implants, to avoid the stress-shielding phenomenon, and to avoid fracture under static and cyclic loadings.[2,3] A low thermal diffusivity is required to protect neighboring bones and/or tissues during implantation.

The Young's modulus of an ideal implant material should be as close to that of the human bone as possible for effective load distribution and to avoid stress shielding.[4−6] Bones have the tendency to grow in the direction of the applied load and build higher strength in the direction of loading.[7,8] The division of load between an implant and the bone depends on their relative Young's moduli. If the Young's modulus of the implant is higher than that of the bone, the load is primarily applied on the implant, and the neighboring bone weakens over time as it experiences little or no loading. The greater the difference between the Young's moduli, the greater the stress shielding and the faster the bone weakens. As a result, the bond between the implant and the bone weakens, thereby leading to aseptic loosening and fracture.[9−16] Most of the currently used implant materials are stiffer than bones, and stress shielding occurs almost invariably.[3]

Polymeric biomaterials and polymer composites are used in various biomedical applications because of their biocompatibility and bioactivity; however, they possess poor mechanical properties.[17] The use of ceramics (alumina and calcium phosphates)[18] has also been explored for such applications, mainly due to their high biocompatibility, bioactivity, high hardness, high compressive strength, and wear resistance,[19−22] but they display inherent limitations of poor fracture toughness and a high Young's modulus.[23−26] Also, 316L stainless steel,[27−30] cobalt−chrome alloys,[27,31] and titanium and its alloys[27,31−34] are the commonly explored metallic systems for

**Received:** April 14, 2022
**Accepted:** July 20, 2023
**Published:** January 5, 2023

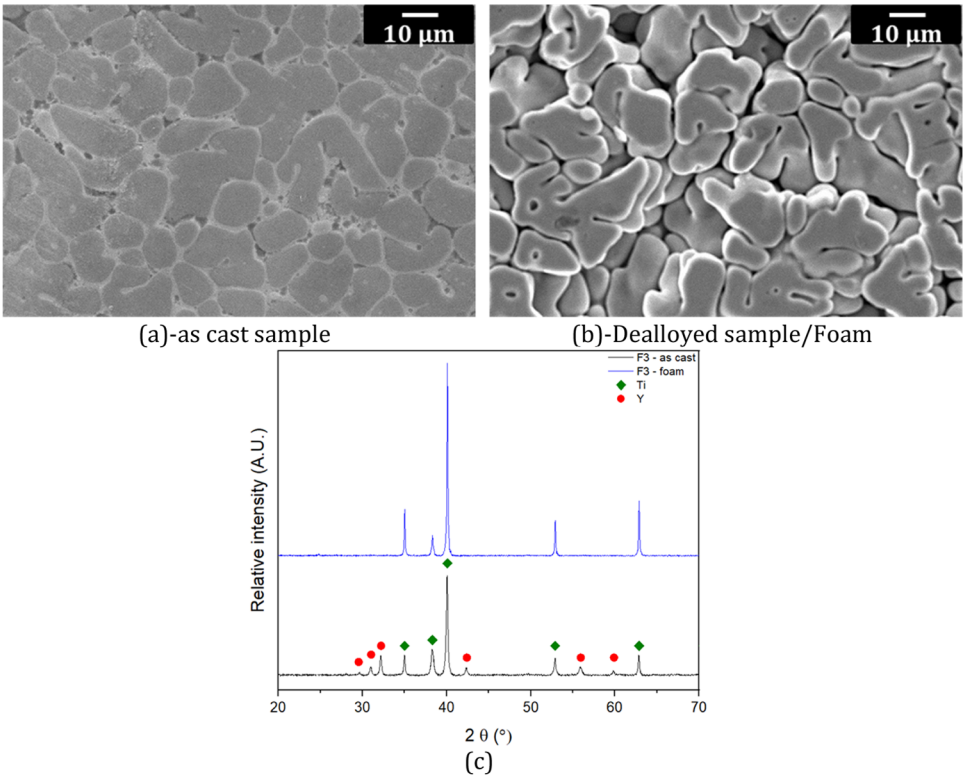


**Figure 1.** SEM images and XRD results of the as-cast and dealloyed Ti-15 atom % Y (F3) sample: (a) SEM of the as-cast sample; (b) SEM of the dealloyed sample/foam; (c) XRD results of the as-cast and dealloyed samples.

implant applications. Corrosion resistance, ease of availability, and ease of fabrication make stainless steel the most widely used biomaterial, but it possesses a high Young's modulus (193 GPa).[23,27,35−37] Cobalt−chrome alloy systems (CoCrWNi and CoNiCrMo) are preferred for high load-bearing applications because of their high tensile strengths (793−860 MPa), but their Young's moduli (210−232 GPa) are even higher than that of stainless steel.[23,27,31,35,36,38−40]

Titanium and its alloys show a high degree of biocompatibility,[29,41] high tensile strength (pure titanium: 550 MPa),[42] and a relatively lower range of Young's modulus (pure titanium: 110 GPa),[1,27,31,43−45] which is still too high when compared with that of the cortical bone.[23,27,36,46−48] Titanium can be an ideal candidate for implant applications provided its Young's modulus could be brought further closer to that of the human bone. Introduction of porosity may help in reducing its Young's modulus.[49] Different methods have been previously used for the development of titanium foams, which include melt infiltration,[50,51] space holders,[52−56] replication,[57,58] bubble generation,[59−62] freeze casting,[63−65] and rapid prototyping.[66−71] A method that provides accurate control of the volume fraction of pores, pore morphology, pore size, and pore interconnectivity needs to be developed.

In the proposed project, we aim at developing a novel method for the development of three-dimensional (3D) interconnected microporous Ti foams. Besides the reduction of the elastic modulus, the introduction of porosity may help in increasing the capability of bone in-growth and introducing high roughness and a relatively high coefficient of friction, which may help in implant fixation with the tissues.

## EXPERIMENTAL PROCEDURES

Titanium and yttrium pellets with purity >99.95% were used as raw materials for the preparation of Ti−Y alloys by arc melting under an argon atmosphere. Titanium and yttrium have high affinity toward oxygen. To reduce the chances of oxidation of raw materials during melting, a vacuum level of $2 \times 10^{-5}$ mbar was attained before the introduction of high-purity argon (99.999%). Before the melting of Ti−Y alloys, the titanium getter was melted to absorb any traces of oxygen. Each sample was melted five times and flipped over after each melting to ensure chemical homogeneity. The weight loss of samples during melting was measured and was found to be less than 0.5%. Electrochemical dealloying for the selective dissolution of yttrium was carried out by immersing the prepared samples in concentrated $HNO_3$ for 24 h, and the weight loss of each sample was recorded as a function of time. Each sample was thoroughly cleaned by ultrasonication in water and in ethanol, followed by drying at 100 °C. Microstructural characterization of the as-cast and de-alloyed samples was performed by scanning electron microscopy (SEM) (JEOL-JSM 6490A). Standard metallographic procedures were employed for the surface preparation of the samples for SEM analysis. Crystal structure characterization of these samples was performed using a Philips diffractometer (Bragg−Brentano geometry), which was equipped with a monochromatic Cu K$\alpha$ radiation. Compression tests were conducted using a Shimadzu universal testing machine at a strain rate of $10^{-4}$ mm/min. Samples for the compression test were cut using an electric discharge machine (EDM) wire cutter and polished afterward to acquire parallel sides. Circular discs for thermal diffusivity measurements were cut using an electric discharge machine (EDM) wire cutter, polished to obtain perfectly parallel sides, and


https://doi.org/10.1021/acsomega.2c02340
ACS Omega 2023, 8, 1876−1884

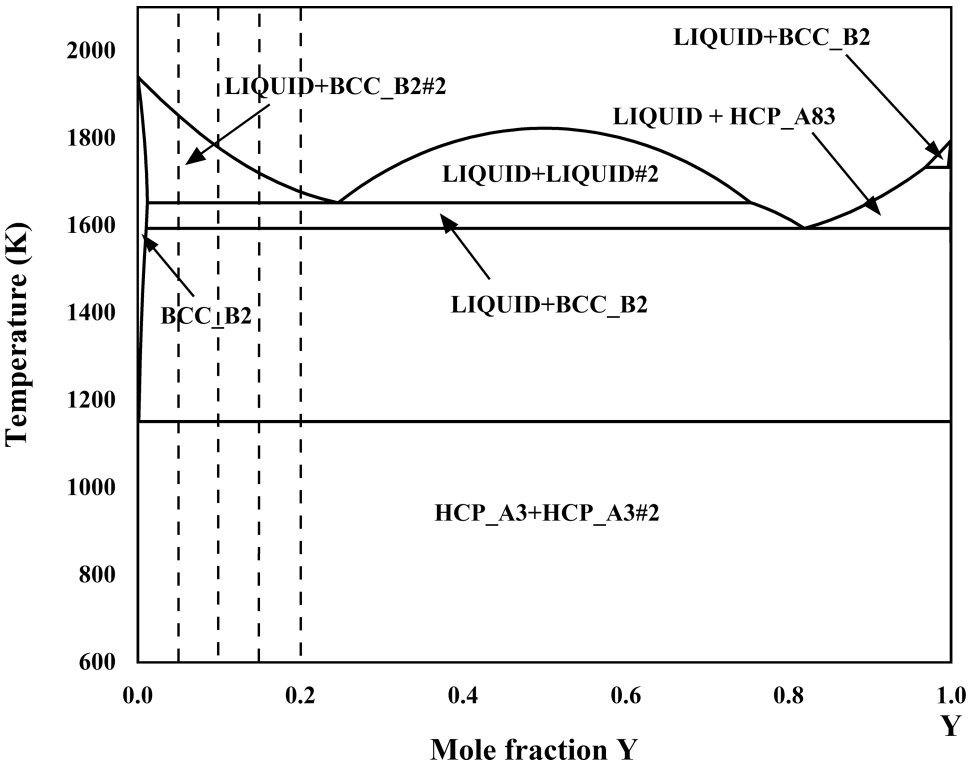


**Figure 2.** Studied compositions (dotted line) superimposed on the Ti−Y phase diagram. Figure adapted from ref 72.

analyzed on a laser flash apparatus at temperatures between 298 and 623 K.

## RESULTS AND DISCUSSION

The present study is dedicated to the development of pure titanium foams by the insertion of a suitable filler metal into titanium metal by melting and its removal by an electrochemical dealloying method. An ideal microstructure for the development of foam by this method should contain titanium as the matrix and the filler element in the interdendritic spaces. Interdendritic areas are interconnected in three dimensions, and therefore, successful removal of the filler element will help in the development of 3D interconnected microporous titanium foams. The choice of the filler element is therefore of utmost importance. It should be soluble in titanium in the liquid state and immiscible in it in the solid state. The filler metal, as a result, will try to separate itself from titanium during solidification and will help in the creation of a titanium-rich matrix with the filler element segregated in the interdendritic areas. The enthalpy of mixing between the titanium and filler elements and the difference in their densities is very important to obtain such a microstructure. The thermodynamic instability of the filler vis-à-vis matrix element is important for its removal by the electrochemical dealloying method for the development of titanium foam. The enthalpy of mixing between Ti and the filler metal should be high enough so that filler metal remains insoluble in titanium in the solid state, but it should not be so high that it separates itself even in the liquid state. Separation of the filler element from titanium is not desirable in the liquid state as it will eventually lead to completely separated zones of titanium and filler metal, and ultimately, the development of foam by electrochemical dealloying will not be possible. The density of the filler metal is also very important. A large difference in the density of the filler metal and titanium may facilitate their separation in the liquid state and result in completely separated zones of the two metals after solidification. The filler metal therefore should have a moderately positive enthalpy of mixing with titanium and a density similar to that of titanium. A judicious selection of the filler metal is required for the successful development of the desired microstructure. Ti has been found to possess a positive enthalpy of mixing with some alkali metals (Cs), alkaline earth metals (Ba), lanthanides (La, Ce, Pr), and actinides (Th, Pu), but they either have a very large difference in density with respect to titanium or have a strongly positive enthalpy of mixing with titanium. Yttrium has been found to possess a moderately positive enthalpy of mixing with titanium and its density is also close to that of titanium. It was therefore decided to employ yttrium as the filler metal for the development of the desired microstructure and for the development of titanium foam.

A Ti-15 atom% Y alloy was prepared by arc melting under an argon atmosphere to verify the aforementioned hypothesis. Scanning electron microscopy of the as-cast sample, shown in Figure 1a, reveals a microstructure that consists of a titanium matrix, whereas yttrium was found to segregate to the interdendritic areas. X-ray diffractometry (XRD) analysis of the as-cast sample revealed the presence of peaks corresponding to pure titanium and pure yttrium. Lattice parameters of Ti and Y were found to be similar to those of pure Ti and Y, respectively, thereby confirming their insolubility in each other in the solid state. SEM analysis of the as-cast samples confirmed the development of the desired microstructure for the further development of titanium foam by the electrochemical dealloying method. The standard equilibrium potential of $Y^{3+}/Y$ (−2.372 SHE) is more negative than that of $Ti^{2+}/Ti$ (−1.63 SHE), and it can be easily removed from the developed alloy by the electrochemical dealloying method. The


https://doi.org/10.1021/acsomega.2c02340
ACS Omega 2023, 8, 1876−1884

**Table 1. Selected Compositions and Their Densities**

| | composition (atom %) | | composition (weight %) | | density of sample (g/cm$^3$) | | porosity (%) |
|---|---|---|---|---|---|---|---|
| name of sample | Ti | Y | Ti | Y | as-cast ($d_1$) | de-alloyed ($d_2$) | $(d_2 - d_1)/d_2) \times 100$ |
| F1 | 95 | 5 | 91.10 | 8.90 | 4.450 | 4.093 | 8.02 |
| F2 | 90 | 10 | 82.90 | 17.10 | 4.536 | 3.781 | 16.64 |
| F3 | 85 | 15 | 75.32 | 24.68 | 4.489 | 3.438 | 23.41 |
| F4 | 80 | 20 | 68.30 | 31.70 | 4.471 | 3.088 | 30.93 |

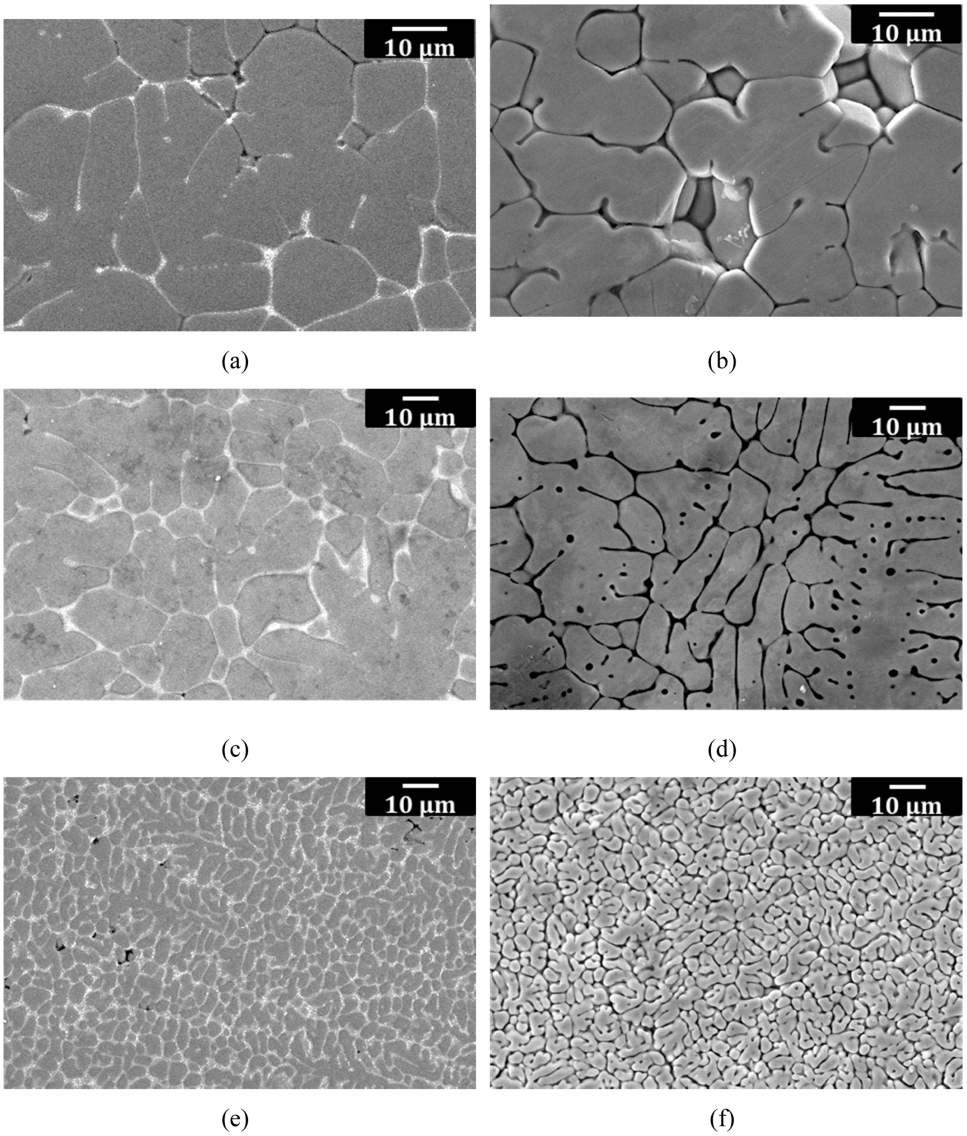


**Figure 3.** SEM images of the (a) as-cast F1, (b) F1 foam, (c) as-cast F2, (d) F2 foam, (e) as-cast F4, and (f) F4 foam samples.

developed alloy was therefore immersed in nitric acid for the selective dissolution of yttrium. SEM and XRD analyses of samples were carried out after immersion in nitric acid to study the effect of the electrochemical dealloying process on the microstructure. An SEM image of the dealloyed sample, shown in Figure 1b, confirms removal from the interdendritic areas, resulting in the development of interdendritic porosity on the surface of the sample. XRD analysis of the dealloyed sample, shown in Figure 1c, reveals the presence of peaks corresponding to pure titanium, whereas peaks corresponding to the presence of yttrium were not observed. It was therefore concluded that dealloying resulted in the complete removal of yttrium not only from the surface but also from the interior of the sample. Complete removal of yttrium was possible only if yttrium-rich areas were interconnected in three dimensions. It was therefore concluded that the successful removal of yttrium from the interconnected interdendritic areas led to the development of the 3D interconnected open cell porous titanium foam. SEM analysis of the de-alloyed samples is shown in Figure 1b, which confirms the presence of interconnected porosity. It was therefore concluded that the proposed method can be used for the development of 3D interconnected microporous titanium foams.

The level of porosity that can be obtained in the titanium foam through this method is related to the amount of yttrium present in the alloy and its successful removal through


https://doi.org/10.1021/acsomega.2c02340
ACS Omega 2023, 8, 1876−1884

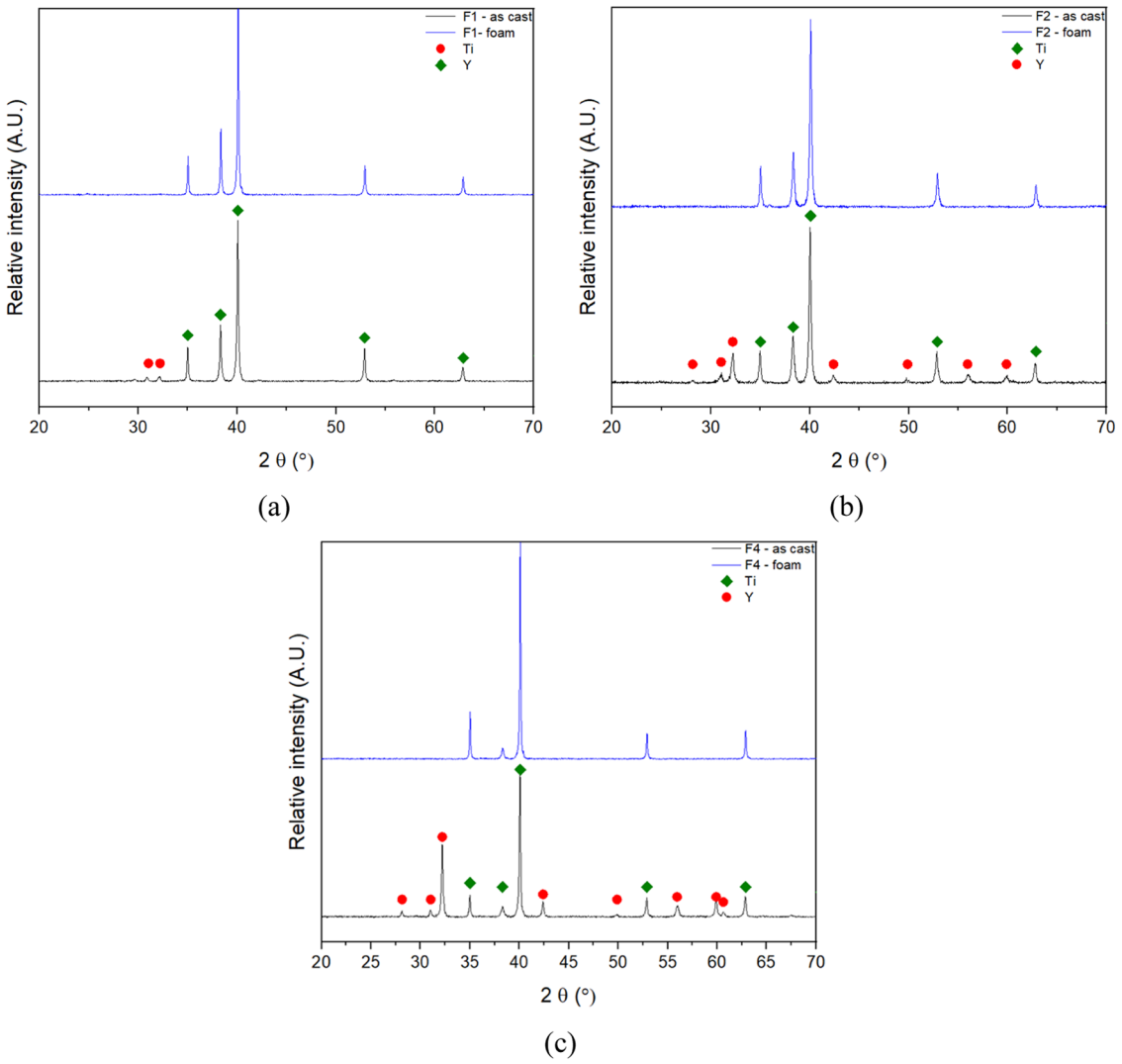


**Figure 4.** X-ray diffraction patterns of as-cast alloys and their respective foams after electrochemical dealloying: (a) F1, (b) F2, and (c) F4 samples.

electrochemical dealloying. To evaluate the effect of increasing amounts of yttrium on the pore morphology and distribution, Ti−Y alloys with varying amounts of yttrium were prepared by arc melting under an argon atmosphere. The Ti−Y phase diagram calculated with the help of Thermocalc software using TCHEA database is shown in the Figure 2.

Figure 2 shows that a monotectic reaction may occur at higher concentrations of Y and result in the separation of titanium-rich and yttrium areas in the liquid state. As a result, the microstructure desired for the development of titanium foam by electrochemical dealloying may not be obtained. It was therefore decided to maintain the amount of yttrium in the alloy at less than 30 atom %. Ti−Y alloy compositions selected in the present study for the development of titanium foams by electrochemical dealloying are shown as dotted lines in Figure 2 on the Ti−Y phase diagram and are indicated in Table 1. SEM images of the alloys before and after electrochemical dealloying are shown in Figure 3.

Figure 3 shows that foams with different levels of porosity can be successfully obtained by varying the amount of yttrium in the master alloys. The pore morphology and distribution are strongly correlated to the distribution of yttrium in the microstructure, which is dependent on the solidification path of the master alloys. Figure 2 shows that the solidification range decreases by increasing the amount of yttrium in the alloys (up to 30 atom % Y). As a result, the microstructure of the alloys changed from coarse to fine, the pore size decreased, and the pore distribution became more homogeneous. This change in the microstructure is evident from the images shown in Figure 3. XRD patterns of the same samples before and after electrochemical dealloying are shown in Figure 4.

XRD analysis of the sample before and after dealloying confirmed the complete removal of yttrium from the matrix. It is therefore concluded that Ti foams with different levels of porosities and pore sizes can be obtained by varying the amount of yttrium in the master alloys.

Thermal diffusivity and compression test measurements were performed to evaluate the effect of the increase in porosity on the thermal and mechanical properties of the developed titanium foams. Circular discs were cut out of the samples using an EDM wire cutter and were polished to obtain the desired level of surface flatness and thickness for thermal diffusivity. Results of thermal diffusivity of the developed foams as a function of temperature are shown in Figure 5.

Figure 5 shows that the thermal diffusivity of the samples decreased with an increasing amount of porosity. The decrease in thermal diffusivity was attributed to the increasing amount of air in the samples and its low thermal diffusivity. The low



https://doi.org/10.1021/acsomega.2c02340
ACS Omega 2023, 8, 1876−1884

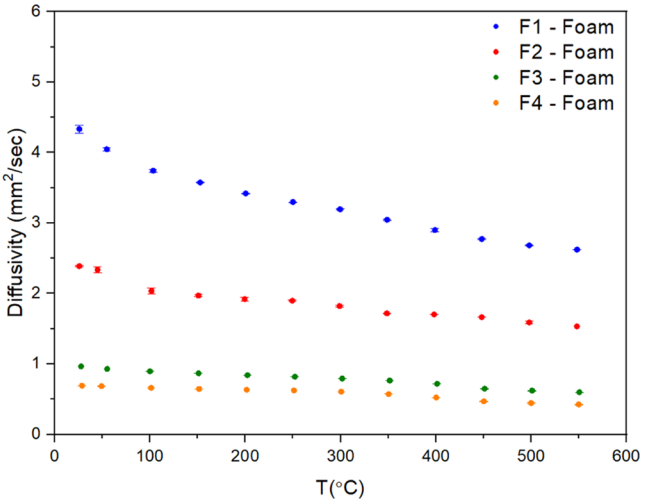


**Figure 5.** Variation of the thermal diffusivity of the developed foams with temperature.

thermal diffusivity of the developed titanium foams makes them suitable for dental implant applications. Compression tests were carried out to evaluate the effect of the volume of porosity on the mechanical properties of the developed titanium foams. Samples for the compression test were prepared using an EDM wire cutter. The stress−strain curve of titanium foams and variation of the yield strength and Young's modulus as a function of the amount of porosity are shown in Figure 6.

Figure 6 shows that the yield strength and elastic modulus of the developed Ti foams decreased with an increase in the level of porosity. The yield strength of the developed Ti foams (1503 MPa > yield strength > 170.3 MPa) is in the range of the strength of the cortical bone (100−230 MPa).[73] The elastic modulus of the developed foam (16.18 GPa > elastic modulus > 38.05 GPa) was also found to be in the range of the elastic modulus of the cortical bone (7−30 GPa).[73] Mechanical properties of the developed foams are in the range of the cortical bone and can be ideal materials for orthopedic implants to overcome/minimize problems of stress shielding. The proposed method can be used for the development of titanium foams with a broad spectrum of mechanical properties by varying the amount of filler elements and resulting levels of porosities. A comparison of the yield strength and Young's modulus of the titanium foams developed in the present study with different biomaterials is shown in Figure 7.

In contrast to previously developed biomaterials, the mechanical properties of the titanium foams developed in

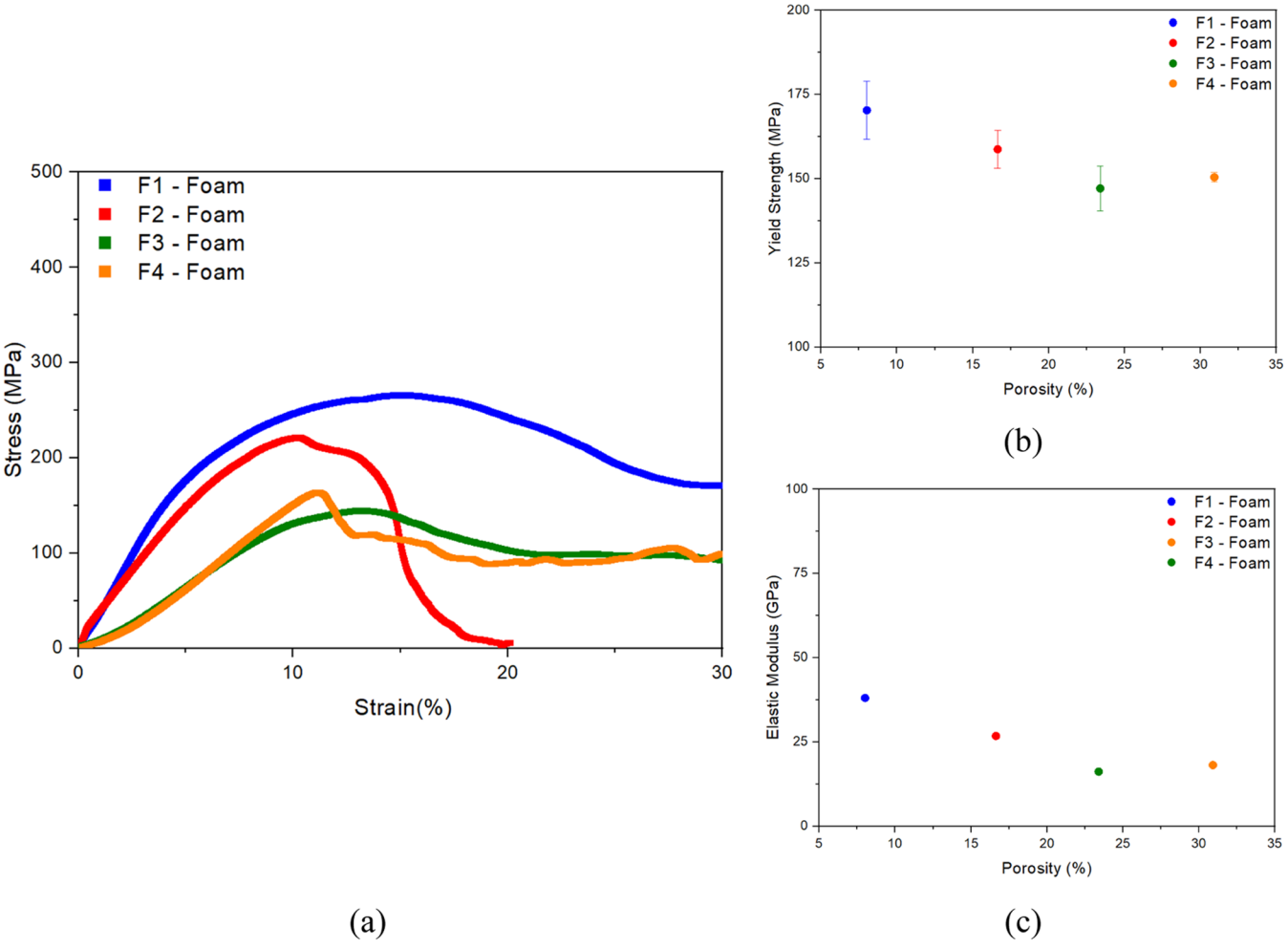


**Figure 6.** (a) Stress−strain curves of the developed foams. (b) Variation of the yield strength as a function of porosity. (c) Variation of the elastic modulus as a function of porosity.



https://doi.org/10.1021/acsomega.2c02340
ACS Omega 2023, 8, 1876−1884

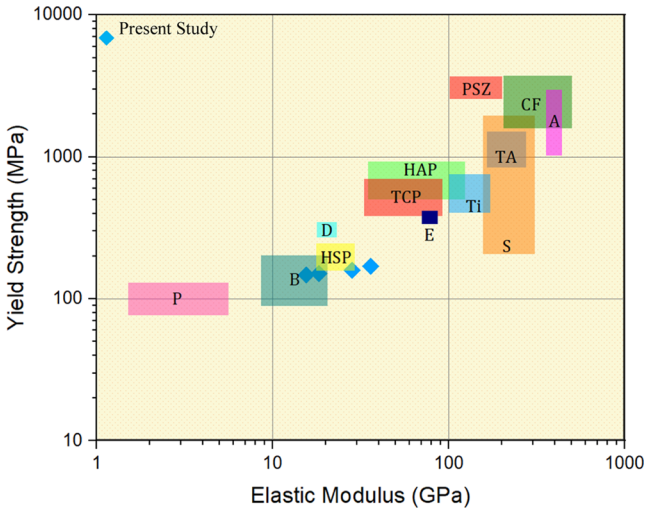


**Figure 7.** Variation of yield strength as a function of the elastic modulus of different materials including foams prepared in the present study (A, alumina; PSZ, partially stabilized zirconia; CF, carbon fiber; TA, titanium alloys; S, 304-series stainless steel; Ti, commercially pure titanium; HAP, hydroxyapatite; TCP, tricalcium phosphate; E, enamel; D, dentin; HSP, high-strength polymer; B, bone; P, polymeric materials). Figure adapted from ref 74.

the present study are in a range similar to that of human bones, in general, and cortical bones, in particular. The method proposed in the present study therefore possesses extreme utility for the development of Ti foams capable of overcoming the problem of stress shielding in orthopedic implants.

In addition to obtaining the desired set of mechanical properties in the developed titanium foams, the method proposed in the present study offers several advantages over previously used methods. The space holder method[75−77] has been considered as one of the most suitable methods for the development of titanium foams. The microstructure and mechanical properties of the foams developed by this method are strongly dependent on a number of variables, which include the size and shape of the space holder particles, compacting pressure, sintering temperature, etc. The space holder method generally results in a closed-cell morphology, nonhomogeneous distribution of pores, and anisotropic mechanical properties. The replication method has also been used for the development of titanium foams; however, the average pore size of the developed foams was very coarse (>500 $\mu$m), which severely degraded their mechanical properties.[75] Foams developed by the replication method also possessed anisotropic properties. Bubble generation methods and freeze-casting methods[64] have also been used for the development of titanium foams; however, they offer reduced pore connectivity, require a complicated experimental setup, and are more prone to contamination. In contrast to the aforementioned methods, the method proposed in the present study provides accurate control of the volume of pores, 3D pore connectivity at very low levels of porosity, microstructural homogeneity, and isotropic mechanical properties. The proposed method requires a very simple experimental setup, involving the use of a melting furnace for the insertion of the filler element and immersion in acid for its removal for the development of interconnected porosity.

## CONCLUSIONS

- A novel method for the development of titanium foams that provides accurate control of the volume fraction of pores, 3D pore connectivity at very low levels of porosity, microstructural homogeneity, and isotropic mechanical properties has been proposed.
- Microstructural and crystal structure results of as-cast samples confirmed the insertion of the filler metal only in the interdendritic areas of the titanium matrix. The filler metal was successfully leached out later by the electrochemical dealloying process, leaving behind a 3D interconnected network of micropores in the titanium matrix.
- Titanium foams with different levels of porosities were successfully prepared and mechanically and thermally characterized.
- Mechanical properties of the developed titanium foams were found to be in the range of the mechanical properties of cortical bones, thereby making them ideal materials for orthopedic implant applications.
- The developed titanium foams showed significantly lower values of thermal diffusivity in comparison with their solid counterparts, thereby pointing out their suitability for dental implant applications.

## AUTHOR INFORMATION


### Corresponding Author

**Khurram Yaqoob** − *School of Chemical and Materials Engineering, National University of Sciences and Technology, 44000 Islamabad, Pakistan;* orcid.org/0000-0003-4208-9018; Email: Khurram.yaqoob@scme.nust.edu.pk

### Authors

**Izza Amjad** − *School of Chemical and Materials Engineering, National University of Sciences and Technology, 44000 Islamabad, Pakistan*

**Muhammad Awais Munir Awan** − *School of Chemical and Materials Engineering, National University of Sciences and Technology, 44000 Islamabad, Pakistan*

**Usman Liaqat** − *School of Chemical and Materials Engineering, National University of Sciences and Technology, 44000 Islamabad, Pakistan;* orcid.org/0000-0001-5798-9890

**Muhammad Zahoor** − *Dept. Molecular Medicine, University of Oslo, 0315 Oslo, Norway*

**Muhammad Kashif** − *Mechanical Engineering Department, University of Central Punjab, 54000 Lahore, Pakistan*

Complete contact information is available at: https://pubs.acs.org/10.1021/acsomega.2c02340


### Notes

The authors declare no competing financial interest.

The datasets generated and/or analyzed in the current study are not publicly available because they are a part of an ongoing funded project, but they are available from the corresponding author on reasonable request.

## ACKNOWLEDGMENTS

Financial support from the Higher Education Commission of Pakistan (HEC, NRPU-6019) and Pakistan Science Foundation (PSF/CRP/Consrm-(732)) is acknowledged.



https://doi.org/10.1021/acsomega.2c02340
ACS Omega 2023, 8, 1876−1884

## REFERENCES


(1) Long, M.; Rack, H. J. Titanium alloys in total joint replacement—a materials science perspective. *Biomaterials* **1998**, *19*, 1621−1639.
(2) Abdel-Hady Gepreel, M.; Niinomi, M. Biocompatibility of Ti-alloys for long-term implantation. *J. Mech. Behav. Biomed. Mater.* **2013**, *20*, 407−415.
(3) Chen, Q.; Thouas, G. A. Metallic implant biomaterials. *Mater. Sci. Eng., R* **2015**, *87*, 1−57.
(4) Robertson, D. M.; Pierre, L. S.; Chahal, R. Preliminary observations of bone ingrowth into porous materials. *J. Biomed. Mater. Res.* **1976**, *10*, 335−344.
(5) Cameron, H. U.; Macnab, I.; Pilliar, R. M. A porous metal system for joint replacement surgery. *Int. J. Artif. Organs* **1978**, *1*, 104−109.
(6) Head, W. C.; Bauk, D. J.; Emerson, R. H., Jr Titanium as the material of choice for cementless femoral components in total hip arthroplasty. *Clin. Orthop. Relat. Res.* **1995**, 85−90.
(7) Hart, N. H.; Nimphius, S.; Rantalainen, T.; Ireland, A.; Siafarikas, A.; Newton, R. U. Mechanical basis of bone strength: influence of bone material, bone structure and muscle action. *J. Musculoskeletal Neuronal Interact.* **2017**, *17*, 114−139.
(8) Singh, R.; Lee, P. D.; Dashwood, R. J.; Lindley, T. C. Titanium foams for biomedical applications: a review. *Mater. Technol.* **2010**, *25*, 127−136.
(9) Rack, H. J.; Qazi, J. I. Titanium alloys for biomedical applications. *Mater. Sci. Eng., C* **2006**, *26*, 1269−1277.
(10) Niinomi, M.; Nakai, M.; Hieda, J. Development of new metallic alloys for biomedical applications. *Acta Biomater.* **2012**, *8*, 3888−3903.
(11) Sumner, D.; Turner, T.; Igloria, R.; Urban, R.; Galante, J. O. Functional adaptation and ingrowth of bone vary as a function of hip implant stiffness. *J. Biomech.* **1998**, *31*, 909−917.
(12) Van Loon, C. J.; de Waal Malefijt, M. C.; Buma, P.; Verdonschot, N.; Veth, R. P. Femoral bone loss in total knee arthroplasty. A review. *Acta Orthop. Belg.* **1999**, *65*, 154−163.
(13) Gross, S.; Abel, E. W. A finite element analysis of hollow stemmed hip prostheses as a means of reducing stress shielding of the femur. *J. Biomech.* **2001**, *34*, 995−1003.
(14) Hrabe, N. W. Characterization of cellular titanium for biomedical applications. Ph.D. Thesis, University of Washington, 2010.
(15) Huiskes, R.; Weinans, H.; van Rietbergen, B. The relationship between stress shielding and bone resorption around total hip stems and the effects of flexible materials. *Clin. Orthop. Relat. Res.* **1992**, *274*, 124−134.
(16) Bauer, T. W.; Schils, J. The pathology of total joint arthroplasty.II. Mechanisms of implant failure. *Skeletal Radiol.* **1999**, *28*, 483−97.
(17) Hutmacher, D. W. Scaffolds in tissue engineering bone and cartilage. *Biomaterials* **2000**, *21*, 2529−2543.
(18) White, E. W.; Weber, J. N.; Roy, D. M.; Owen, E. L.; Chiroff, R. T.; White, R. A. Replamineform porous biomaterials for hard tissue implant applications. *J. Biomed. Mater. Res.* **1975**, *9*, 23−27.
(19) De Groot, K. Bone induction by allogenous rat dentine implanted subcutaneously. *Arch. Oral Biol.* **1974**, *19*, 477−9.
(20) Jarcho, M.; Bolen, C. H.; Thomas, M. B.; Bobick, J.; Kay, J. F.; Doremus, R. H. Hydroxylapatite synthesis and characterization in dense polycrystalline form. *J. Mater. Sci.* **1976**, *11*, 2027−2035.
(21) Akao, M.; Aoki, H.; Kato, K. Mechanical properties of sintered hydroxyapatite for prosthetic applications. *J. Mater. Sci.* **1981**, *16*, 809−812.
(22) El-Ghannam, A. Bone reconstruction: from bioceramics to tissue engineering. *Expert Rev. Med. Devices* **2005**, *2*, 87−101.
(23) Navarro, M.; Michiardi, A.; Castaño, O.; Planell, J. A. Biomaterials in orthopaedics. *J. R. Soc. Interface* **2008**, *5*, 1137−1158.
(24) Ogino, M.; Ohuchi, F.; Hench, L. L. Compositional dependence of the formation of calcium phosphate films on bioglass. *J. Biomed. Mater. Res.* **1980**, *14*, 55−64.
(25) Schepers, E.; de Clercq, M.; Ducheyne, P.; Kempeneers, R. Bioactive glass particulate material as a filler for bone lesions. *J. Oral Rehabil.* **2008**, *18*, 439−452.
(26) Stanley, H. R.; Hall, M. B.; Clark, A. E.; King, C. J., 3rd; Hench, L. L.; Berte, J. J. Using 45S5 bioglass cones as endosseous ridge maintenance implants to prevent alveolar ridge resorption: a 5-year evaluation. *Int. J. Oral Maxillofac. Implants* **1997**, *12*, 95−105.
(27) Geetha, M.; Singh, A. K.; Asokamani, R.; Gogia, A. K. Ti based biomaterials, the ultimate choice for orthopaedic implants − A review. *Prog. Mater. Sci.* **2009**, *54*, 397−425.
(28) Escalas, F.; Galante, J.; Rostoker, W.; Coogan, P. Biocompatibility of materials for total joint replacement. *J. Biomed. Mater. Res.* **1976**, *10*, 175−195.
(29) Lemons, J. E.; Niemann, K. M. W.; Weiss, A. B. Biocompatibility studies on surgical-grade titanium-, cobalt-, and iron-base alloys. *J. Biomed. Mater. Res.* **1976**, *10*, 549−553.
(30) Syrett, B. C.; Davis, E. E. In vivo evaluation of a high-strength, high-ductility stainless steel for use in surgical implants. *J. Biomed. Mater. Res.* **1979**, *13*, 543−556.
(31) Davis, J. R. *Handbook of Materials for Medical Devices*; ASM International, 2003.
(32) Raducanu, D.; Vasilescu, E.; Cojocaru, V. D.; Cinca, I.; Drob, P.; Vasilescu, C.; Drob, S. I. Mechanical and corrosion resistance of a new nanostructured Ti−Zr−Ta−Nb alloy. *J. Mech. Behav. Biomed. Mater.* **2011**, *4*, 1421−1430.
(33) Tong, Y. X.; Guo, B.; Zheng, Y. F.; Chung, C. Y.; Ma, L. W. Effects of Sn and Zr on the Microstructure and Mechanical Properties of Ti-Ta-Based Shape Memory Alloys. *J. Mater. Eng. Perform.* **2011**, *20*, 762−766.
(34) Niinomi, M.; Minerals, M.; Meeting, M. S.; Minerals, M.; Committee, M. S. S. M.; Minerals, M.; Committee, M. S. T. *Structural Biomaterials for the 21st Century*, Proceedings of the Symposium Sponsored by the SMD Structural Materials and Titanium Committees...[et al.]; Presented at the 2001 TMS Annual Meeting in New Orleans, LA, on February 11−12, 2001; TMS.
(35) Semlitsch, M.; Willert, H. G. Properties of implant alloys for artificial hip joints. *Med. Biol. Eng. Comput.* **1980**, *18*, 511−520.
(36) Davidson, J.; Georgette, F. *State of the Art Materials for Orthopedic Prosthetic Devices*; Society of Manufacturing Engineers, 1987.
(37) Geetha, M.; Singh, A. K.; Asokamani, R.; Gogia, A. K. Ti based biomaterials, the ultimate choice for orthopaedic implants−a review. *Prog. Mater. Sci.* **2009**, *54*, 397−425.
(38) International Agency for Research on Cancer. *Surgical Implants and Other Foreign Bodies*; IARC, 1999; p 409.
(39) Ramsden, J. J.; Allen, D. M.; Stephenson, D. J.; Alcock, J. R.; Peggs, G. N.; Fuller, G.; Goch, G. The Design and Manufacture of Biomedical Surfaces. *CIRP Ann.* **2007**, *56*, 687−711.
(40) Alvarado, J.; Maldonado, R.; Marxuach, J.; Otero, R. Biomechanics of hip and knee prostheses. *Appl. Eng. Mech. Med.* **2003**, 6−22.
(41) Kodama, T. Study on biocompatibility of titanium alloys. *J. Stomatol. Soc., Jpn.* **1989**, *56*, 263−288.
(42) Li, J. C.-M. *Microstructure and Properties of Materials*; World Scientific, 1996; Vol *2*.
(43) Liu, X.; Chu, P. K.; Ding, C. Surface modification of titanium, titanium alloys, and related materials for biomedical applications. *Mater. Sci. Eng., R* **2004**, *47*, 49−121.
(44) Ergül, E.; Özkan Gülsoy, H.; Günay, V. Effect of sintering parameters on mechanical properties of injection moulded Ti−6Al−4V alloys. *Powder Metall.* **2009**, *52*, 65−71.
(45) Nyberg, E.; Miller, M.; Simmons, K.; Weil, K. S. Microstructure and mechanical properties of titanium components fabricated by a new powder injection molding technique. *Mater. Sci. Eng., C* **2005**, *25*, 336−342.
(46) Rho, J.-Y.; Tsui, T. Y.; Pharr, G. M. Elastic properties of human cortical and trabecular lamellar bone measured by nanoindentation. *Biomaterials* **1997**, *18*, 1325−1330.



https://doi.org/10.1021/acsomega.2c02340
*ACS Omega* 2023, 8, 1876−1884

(47) Niinomi, M. Mechanical properties of biomedical titanium alloys. *Mater. Sci. Eng., A* **1998**, *243*, 231−236.
(48) Long, M.; Rack, H. J. Titanium alloys in total joint replacement - A materials science perspective. *Biomaterials* **1998**, *19*, 1621−1639.
(49) Kaya, M.; Yakuphanoğlu, F. A study on microstructure of porous TiNbZr alloy produced as biomaterial. *Materialwiss. Werkstofftech.* **2019**, *50*, 742−746.
(50) Xie, C.; Li, H.; Yuan, B.; Gao, Y.; Luo, Z.; Zhu, M. Ti3Sn−NiTi Syntactic Foams with Extremely High Specific Strength and Damping Capacity Fabricated by Pressure Melt Infiltration. *ACS Appl. Mater. Interfaces* **2019**, *11*, 28043−28051.
(51) Zhao, Y.; Tao, X.; Xue, X. Manufacture and mechanical properties of metal matrix syntactic foams. *Mater. Sci. Technol.* **2008**, *4*, 2607−2615.
(52) Wen, C.; Yamada, Y.; Shimojima, K.; Chino, Y.; Hosokawa, H.; Mabuchi, M. Novel titanium foam for bone tissue engineering. *J. Mater. Res.* **2002**, *17*, 2633−2639.
(53) Müller, U.; Imwinkelried, T.; Horst, M.; Sievers, M.; Graf-Hausner, U. Do human osteoblasts grow into open-porous titanium. *Eur. Cells Mater.* **2006**, *11*, 8−15.
(54) Bram, M.; Stiller, C.; Buchkremer, H. P.; Stöver, D.; Baur, H. High-porosity titanium, stainless steel, and superalloy parts. *Adv. Eng. Mater.* **2000**, *2*, 196−199.
(55) Singh, R.; Lee, P. D.; Lindley, T. C.; Dashwood, R. J.; Ferrie, E.; Imwinkelried, T. Characterization of the structure and permeability of titanium foams for spinal fusion devices. *Acta Biomater.* **2009**, *5*, 477−487.
(56) Niu, W.; Bai, C.; Qiu, G.; Wang, Q.; Wen, L.; Chen, D.; Dong, L. Preparation and characterization of porous titanium using space-holder technique. *Rare Met.* **2009**, *28*, 338−342.
(57) Ye, B.; Dunand, D. C. Titanium foams produced by solid-state replication of NaCl powders. *Mater. Sci. Eng., A* **2010**, *528*, 691−697.
(58) Frenkel, S. R.; Jaffe, W. L.; Dimaano, F.; Iesaka, K.; Hua, T. Bone response to a novel highly porous surface in a canine implantable chamber. *J. Biomed. Mater. Res.* **2004**, *71B*, 387−391.
(59) Kearns, M. W.; Blenkinsop, P.; Barber, A. C.; Farthing, T. Manufacture of a novel porous metal. *Int. J. Powder Metall.* **1988**, *24*, 59−64.
(60) Higuchi, Y.; Ohashi, Y.; Nakajima, H. Biocompatibility of Lotus-type Stainless Steel and Titanium in Alveolar Bone. *Adv. Eng. Mater.* **2006**, *8*, 907−912.
(61) Greiner, C.; Oppenheimer, S. M.; Dunand, D. C. High strength, low stiffness, porous NiTi with superelastic properties. *Acta Biomater.* **2005**, *1*, 705−716.
(62) Oppenheimer, S. M.; Dunand, D. C. Porous NiTi by creep expansion of argon-filled pores. *Mater. Sci. Eng., A* **2009**, *523*, 70−76.
(63) Fife, J.; Li, J.; Dunand, D.; Voorhees, P. W. Morphological analysis of pores in directionally freeze-cast titanium foams. *J. Mater. Res.* **2009**, *24*, 117−124.
(64) Chino, Y.; Dunand, D. C. Directionally freeze-cast titanium foam with aligned, elongated pores. *Acta Mater.* **2008**, *56*, 105−113.
(65) Deville, S. Freeze-casting of porous biomaterials: structure, properties and opportunities. *Materials* **2010**, *3*, 1913−1927.
(66) Lopez-Heredia, M. A.; Goyenvalle, E.; Aguado, E.; Pilet, P.; Leroux, C.; Dorget, M.; Weiss, P.; Layrolle, P. Bone growth in rapid prototyped porous titanium implants. *J. Biomed. Mater. Res.* **2008**, *85A*, 664−673.
(67) Xue, W.; Krishna, B.; Bandyopadhyay, A.; Bose, S. Processing and biocompatibility evaluation of laser processed porous titanium. *Acta Biomater.* **2007**, *3*, 1007−1018.
(68) Mullen, L.; Stamp, R. C.; Brooks, W. K.; Jones, E.; Sutcliffe, C. J. Selective Laser Melting: A regular unit cell approach for the manufacture of porous, titanium, bone in-growth constructs, suitable for orthopedic applications. *J. Biomed. Mater. Res., Part B* **2009**, *89B*, 325−334.
(69) Hollander, D. A.; Von Walter, M.; Wirtz, T.; Sellei, R.; Schmidt-Rohlfing, B.; Paar, O.; Erli, H.-J. Structural, mechanical and in vitro characterization of individually structured Ti−6Al−4V produced by direct laser forming. *Biomaterials* **2006**, *27*, 955−963.
(70) Heinl, P.; Rottmair, A.; Körner, C.; Singer, R. F. Cellular titanium by selective electron beam melting. *Adv. Eng. Mater.* **2007**, *9*, 360−364.
(71) Li, J. P.; de Wijn, J. R.; Van Blitterswijk, C. A.; de Groot, K. Porous Ti6Al4V scaffold directly fabricating by rapid prototyping: preparation and in vitro experiment. *Biomaterials* **2006**, *27*, 1223−1235.
(72) *Thermo-Calc Software [TCHEA4]*, (accessed 1-8-2022).
(73) Kokubo, T.; Kim, H.-M.; Kawashita, M. Novel bioactive materials with different mechanical properties. *Biomaterials* **2003**, *24*, 2161−2175.
(74) Oshida, Y.; Tuna, E. B.; Aktören, O.; Gençay, K. Dental implant systems. *Int. J. Mol. Sci.* **2010**, *11*, 1580−678.
(75) Niu, W.; Bai, C.; Qiu, G.; Wang, Q. Processing and properties of porous titanium using space holder technique. *Mater. Sci. Eng., A* **2009**, *506*, 148−151.
(76) Wen, C. E.; Yamada, Y.; Shimojima, K.; Chino, Y.; Asahina, T.; Mabuchi, M. Processing and mechanical properties of autogenous titanium implant materials. *J. Mater. Sci.: Mater. Med.* **2002**, *13*, 397−401.
(77) Wen, C.; Mabuchi, M.; Yamada, Y.; Shimojima, K.; Chino, Y.; Asahina, T. Processing of biocompatible porous Ti and Mg. *Scr. Mater.* **2001**, *45*, 1147−1153.


https://doi.org/10.1021/acsomega.2c02340
*ACS Omega* 2023, 8, 1876−1884